Journal of Hazardous Materials 171 (2009) 335–339

Contents lists available at ScienceDirect

Journal of Hazardous Materials

journal homepage: www.elsevier.com/locate/jhazmat

Nickel adsorption by sodium polyacrylate-grafted activated carbon

A. Ewecharoen [a], P. Thiravetyan [a,*], E. Wendel [b], H. Bertagnolli [b]

[a] Division of Biotechnology, School of Bioresources and Technology, King Mongkut's University of Technology Thonburi, 83 Moo 8 Thakham, Bangkhuntien, Bangkok 10150, Thailand
[b] Institut für Physikalische Chemie, Universität Stuttgart, Pfaffenwaldring 55, 70569 Stuttgart, Germany

ARTICLE INFO

Article history:
Received 8 April 2009
Received in revised form 1 June 2009
Accepted 3 June 2009
Available online 10 June 2009

Keywords:
Activated carbon
Nickel adsorption
Gamma ray
XAS
FTIR

ABSTRACT

A novel sodium polyacrylate grafted activated carbon was produced by using gamma radiation to increase the number of functional groups on the surface. After irradiation the capacity for nickel adsorption was studied and found to have increased from 44.1 to 55.7 mg g^{-1}. X-ray absorption spectroscopy showed that the adsorbed nickel on activated carbon and irradiation-grafted activated carbon was coordinated with 6 oxygen atoms at 2.04–2.06 Å. It is proposed that this grafting technique could be applied to other adsorbents to increase the efficiency of metal adsorption.

1. Introduction

Heavy metal pollution of waters comes from various industries, such as steel production, mining, electronics, and motor vehicles that have inadequate wastewater management. Excessive levels of heavy metals have been linked with a wide range of health conditions, including skin disease, birth defects and cancer. As a result the World Health Organization has recommended strict controls on the percentages of various heavy metals in effluent waters.

Various techniques (*e.g.* chemical precipitation, electrolysis, ion exchange and membrane filtration) are currently used to treat wastewaters before discharge into the environment [1,2]. An adsorption is another easier and cheaper technique onto solid materials, whereby the adsorbate is accumulated on the surface of or inside an adsorbent. The efficiency of adsorption depends on many factors, including the surface area, pore size distribution, polarity, and functional groups of the adsorbent [3–5]. Cheap adsorbents can be developed for treating wastewaters by various methods, which include hydrolysis [6,7], esterification [7], saponification [8], grafting by chemical methods [9–13] or irradiation by UV or γ-rays [14–17] of abundant natural or waste materials. For example, activated carbon can be used to treat toxic substances, such as nickel [18,19], copper [20,21], zinc [20,22], toluene [22], cyanide [20,23], dyes [24,25] in commercial operations, because of its highly porous structure and large surface area available for adsorption or chemical reaction.

The aim of the present research was to develop a novel activated carbon to treat nickel-contaminated wastewater. Previous work has shown that carboxyl groups are involved in nickel adsorption [26,27] and that the number of functional groups on the surface of sample could be increasing by grafted monomers or polymers on adsorbents. We have also found that the generation of –COONa groups on the surface of coir pith by treatment with sodium hydroxide increased the efficiency of nickel adsorption [27]. In the present work, we report investigations of the effects of γ-radiation on the efficiency of activated carbon grafted with sodium polyacrylate (as polymer) for nickel adsorption, since –COONa should be generated. Measurements of the adsorption capacity, mechanism of adsorption and desorption, Fourier transform infrared spectroscopy (FTIR) and X-ray absorption spectroscopy (XAS) have been used to characterize the adsorbents.

2. Materials

2.1. Activated carbon

The activated carbon used in this work was made by Sigma Chemicals Pty Ltd. It was washed with distilled water and dried in the air, then stored in desiccators to control its moisture content. Sodium polyacrylate (PAAS) produced by Fluka, molecular weight 16,000.

2.2. Preparation of irradiation-grafted activated carbon

Activated carbon (10 g) was soaked with sodium polyacrylate (PAAS) (150 ml) at room temperature for 1 h, after which it was irra-

* Corresponding author. Tel.: +66 2 470 7535; fax: +66 2 452 3455.
E-mail addresses: paitip@hotmail.com, paitip.thi@kmutt.ac.th (P. Thiravetyan).

0304-3894/$ – see front matter © 2009 Elsevier B.V. All rights reserved.
doi:10.1016/j.jhazmat.2009.06.008

diated with gamma rays from a ^{60}Co source (Beta Gamma Service GmbH & Co. KG, Germany) at room temperature with 1.06 kGy h^{-1} until the total received doses were 10 and 20 kGy. The sample was then washed with hot water to remove excess of polymer, and the radiation-grafted activated carbon was dried in the air and stored in desiccators until use.

2.3. Real rinse water from electroplating wastewater

Nickel-rich wastewater (rinse water) with a nickel concentration of 145 mg l^{-1} (pH 3.92) was collected from an electroplating factory located in Samuthprakarn province (Thailand).

3. Methods

3.1. Surface area determination

Surface area (m^2 g^{-1}) was measured by nitrogen porosimetry at 77 K and the Brunauer–Emmet–Teller (BET) equation [28] used to estimate the pore characteristics such as pore diameter and total pore volume (Quantachrome-autosorb). The total pore volume was estimated to be the liquid volume of adsorbate (N_2) at a relative pressure of 0.99.

3.2. Functional groups on the adsorbents

Fourier transform infrared spectroscopy (FTIR, Bruker-Vector 22) was used to identify qualitatively the functional groups on the adsorbents. Spectra were acquired between 4000 and 400 cm^{-1} using the KBr disc technique; samples were ground and well mixed with KBr in a ratio of 1 mg sample to 550 mg KBr and then compressed in the disc.

3.3. Boehm's titration [29]

Boehm's titration was used to calculate the number of acidic surface groups. The adsorbent (1.0 g) was mixed with 50 ml each of 0.1 M NaOH, $NaHCO_3$ and Na_2CO_3, and shaken continuously for 24 h. The supernatants were separated by filtration, and 10 ml of each filtrate used for titration with 0.1 M HCl using methyl orange as an indicator. Potentiometric titration curves were analyzed in the pH range 3–11. Note that NaOH neutralizes carboxyl, lactone and phenolic groups, Na_2CO_3 neutralizes carboxyl and lactone groups and $NaHCO_3$ neutralizes only carboxyl groups.

3.4. Nickel adsorption

The experiments were carried out by using 0.1 g of adsorbents and 10 ml of nickel-rich wastewater. The mixtures were shaken in a flask at 150 rpm for 2 h at room temperature, filtered, and the Ni residue in the supernatants measured using Inductively coupled plasma spectroscopy (ICP-JY124). The saturated adsorbents were dried in air and stored in desiccators until investigation with X-ray absorption spectroscopy (XAS).

The adsorption capacity (q_e) was determined by the following equation:

$$q_e = \frac{(C_0 - C_e) \times V}{W} \quad (1)$$

where C_0 and C_e are the initial and equilibrium Ni concentrations (mg l^{-1}), respectively, V is volume of solution (l), and W is the mass of adsorbent (g).

Nickel uptake was estimated by the Langmuir isotherm:

$$q_e = \frac{q_{\max} k_a C_e}{1 + k_a C_e} \quad (2)$$

Table 1
Percentage of nickel removal by activated carbon and irradiation-grafted activated carbon at 10 and 20 kGy at various adsorbent dosages.

Adsorbent dosage (% w/v)	% Nickel removal		
	Activated carbon	Irradiation-grafted activated carbon	
		10 kGy	20 kGy
1	18.4 ± 1.0	18.8 ± 0.6	29.5 ± 0.3
3	68.0 ± 0.2	68.2 ± 0.2	79.0 ± 0.8
5	82.7 ± 0.1	82.7 ± 0.1	93.9 ± 1.0

Table 2
Surface characteristics of activated carbon and irradiation-grafted activated carbon.

Characteristic	Activated carbon	Irradiation-grafted activated carbon
I. Surface area by nitrogen porosimetry		
Multipoint BET (m^2 g^{-1})	899	892
Total pore volume (cm^3 g^{-1})	0.49	0.49
Average pore diameter (Å)	21.77	21.91
II. Surface oxide (mequiv. g^{-1})		
Carboxyl	0.71 ± 0.04	1.16 ± 0.06
Lactone	3.15 ± 0.16	2.29 ± 0.10
Phenolic	0.46 ± 0.02	0.55 ± 0.03

where k_a is Langmuir constant, q_{max} is indicative of maximum adsorption capacity, q_e is the metal uptake (mg nickel g^{-1} of adsorbent), and C_e is the nickel concentration at equilibrium (mg l^{-1}).

3.5. Desorption

The adsorbents containing Ni were eluted successively with 10 ml of distilled water, 10 ml of 0.0125 M H_2SO_4 and 10 ml of 0.025 M H_2SO_4. Ni concentrations were measured by ICP spectroscopy.

3.6. X-ray absorption spectroscopy (XAS) investigations

XANES and EXAFS measurements at the Ni K-edge (8333 eV) were performed at the beamline X1 of the Hamburger Synchrotronstrahlungslabor (HASYLAB) at DESY in Hamburg, Germany. The samples were measured with a Si(1 1 1) double crystal monochromator in transmission mode. The references and samples were embedded in a cellulose matrix while the samples were added with cellulose and pressed into pellets. The concentrations of the reference samples were adjusted to yield an edge jump of about 1.

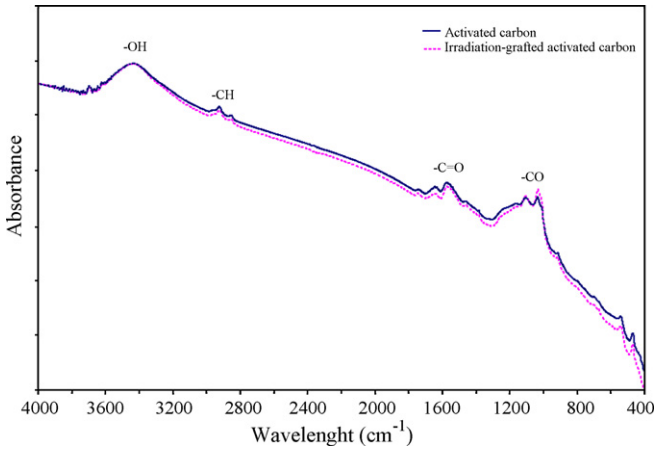

Fig. 1. IR spectra of activated carbon and irradiation-grafted activated carbon.

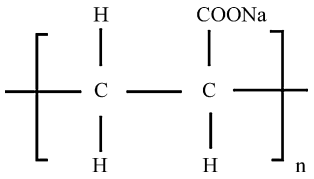

Fig. 2. The structure of sodium polyacrylate.

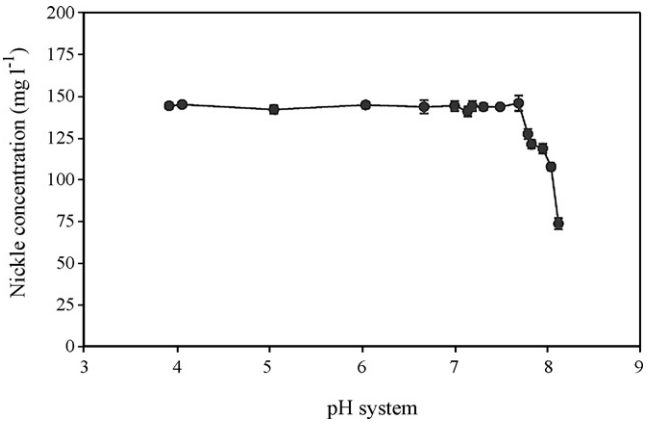

Fig. 3. Effect of pH to nickel precipitation.

However, because of the low nickel content in the samples from the adsorption experiments, the best achievable edge jump for the Ni-spectra was about 0.1–0.2. All experiments were carried out under ambient conditions at 21 °C. Energy calibration was performed with a nickel metal foil.

In the data analysis, the program ATHENA [30,31] was used for pre-edge subtraction and normalization of the experimental spectra. Afterwards, the program AUTOBK [32] was used to remove the post-edge background and to isolate the EXAFS function $\chi(k)$. Curve fitting analysis of the EXAFS function, weighted with k^3, was performed according to the curved wave formalism of the program EXCURV98 [33] with XALPHA phase and amplitude functions. The mean free path of the scattered electrons was calculated from the imaginary part of the potential (VPI set to −4.00), the amplitude reduction factor (AFAC) was fixed at 0.8 and an overall energy shift (E_f) was introduced to give a best fit to the data.

4. Result and discussion

4.1. Characterization of adsorbents

Gamma radiation was used as the initiator for grafting activated carbon with sodium polyacrylate (PAAS). Table 1 shows the effect of total radiation dose values at 10 and 20 kGy for nickel adsorption. It presents nickel removal by irradiated activated carbon at 10 kGy was no difference compared to activated carbon. While, the adsorption by grafted activated carbon at 20 kGy was higher. Therefore, the suitable total radiation dose (20 kGy) can be induced for the radical formation of surface oxide on the acti-

Table 3
Langmuir isotherm showing the efficiency of nickel adsorption by activated carbon and irradiation-grafted activated carbon.

Adsorbents	Langmuir isotherm		
	q_{max} (mg g^{-1})	k_a (l mg^{-1})	r^2
Activated carbon	44.1 ± 0.7	0.005 ± 0.001	0.999
Irradiation-grafted activated carbon	55.7 ± 0.6	0.009 ± 0.001	0.998

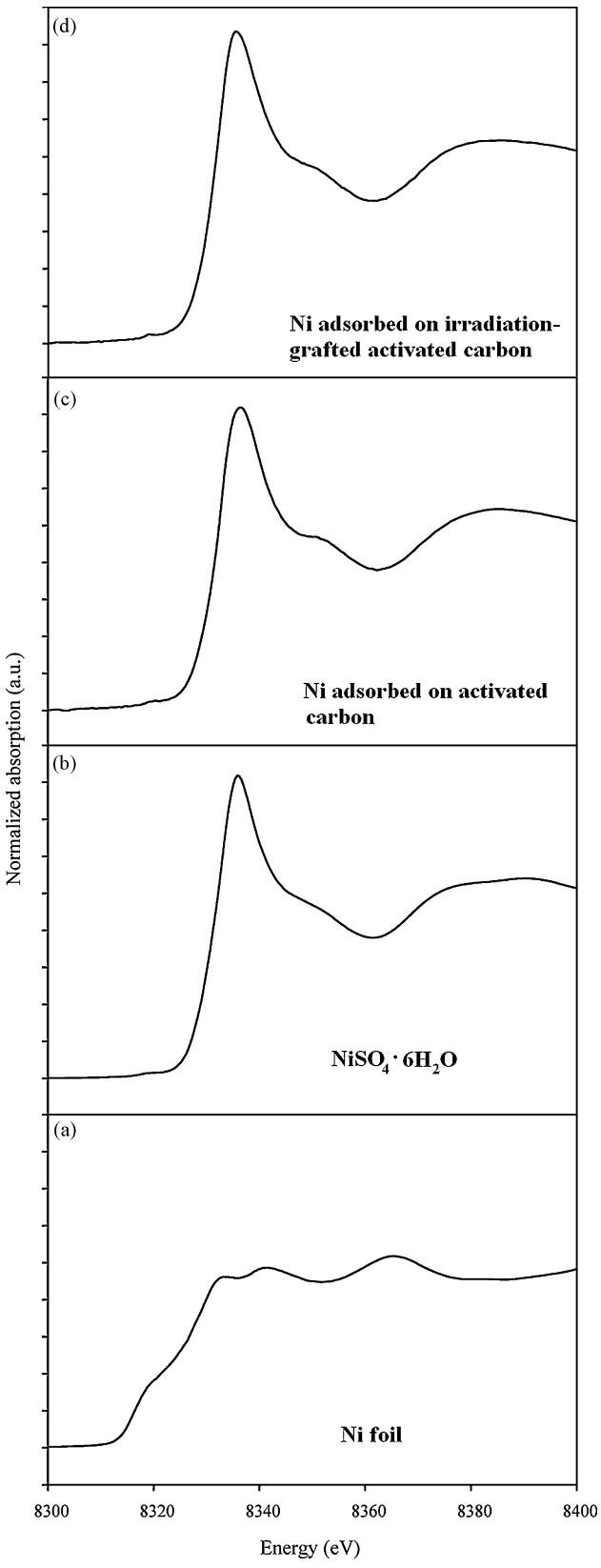

Fig. 4. XANES spectra of nickel adsorbed on activated carbon and irradiation-grafted activated carbon compared with nickel reference standards.

Table 4
Desorption of nickel from nickel-adsorbed activated carbon and nickel-adsorbed irradiation-grafted activated carbon.

Adsorbents	% Nickel desorption			% Total desorption
	I. Distilled water	II. 0.0125 M sulfuric acid	III. 0.025 M sulfuric acid	
Activated carbon	0.8 ± 0.1	87.6 ± 3.1	8.8 ± 0.6	97.2 ± 1.4
Irradiation-grafted activated carbon	0.8 ± 0.2	87.5 ± 1.2	9.3 ± 0.3	97.5 ± 0.6

Table 5
Structure parameters obtained from the XAS analysis of activated carbon and irradiation-grafted activated carbon.

References	A–Bs[a]	N[b,c]	r[d] (Å)	r[d] (Å) XRD[f]	σ[e] (Å)	E_f[f] (eV)	k-range (Å^{-1})	Fit-index
NiO (black)	Ni–O	6	2.07 ± 0.02	2.09	0.077 ± 0.008	8.68	3–12	19.28
	Ni–Ni	12	2.94 ± 0.03	2.95	0.089 ± 0.013			
$NiSO_4{\cdot}6H_2O$	Ni–O	6	2.06 ± 0.02	2.02	0.074 ± 0.007	7.98	3–12	31.51
$NiCO_3$	Ni–O	6	–	2.08	–	–	–	–
	Ni–C	6		2.93				
Activated carbon	Ni–O	6	2.04 ± 0.02	–	0.074 ± 0.007	8.05	3–12	45.09
Irradiation-grafted activated carbon	Ni–O	6	2.05 ± 0.02	–	0.083 ± 0.008	7.76	3–12	45.15

[a] Absorber (A)–backscatterers (Bs).
[b] Coordination number, N.
[c] The fixed multiplicities and crystallographic distances were taken from the following references: NiO (black) [34], $NiSO_4{\cdot}6H_2O$ [35] and $NiCO_3$ [36].
[d] Interatomic distance, r.
[e] Debye–Waller factor, σ.
[f] Edge position, E_f (Fermi energy) relative to calculated vacuum zero.

vated carbon surface that initiates the polymerization of polymer and thus a mixture of graft between activated carbon and sodium polyacrylate is obtained. Table 2 shows the surface characteristics of activated carbon and irradiation-grafted activated carbon as determined by nitrogen porosimetry and Boehm's titration method. No differences were observed between the surface areas of activated carbon and irradiation-grafted activated carbon, but there were appreciable differences in their carboxyl, phenolic and lactone group contents. IR peaks at 1033–1305 cm^{-1}, 1600–1666 cm^{-1} and 3199–3657 cm^{-1} from C–O, C=O and O–H, respectively (Fig. 1), increased as a result of irradiation grafting because of the presence of carboxylate groups in the sodium polyacrylate (Fig. 2) attached to the surface of activated carbon after γ-irradiation.

4.2. Characterization of nickel wastewater

The pH affects to nickel solubility and nickel precipitation was studied under initial pH range of 4–8 (Fig. 3). The concentration of nickel decreased at pH higher than 7.7 because at higher pHs means higher OH^- ions in the solution, that can bind with Ni^{2+} ions to hydroxide complexes form as the nickel hydroxide. Therefore, the system pH should not exceed 7.7.

4.3. Adsorption isotherm study

Maximum values of nickel adsorption (q_{max}) by activated carbon and irradiation-grafted activated carbon fitted to Langmuir isotherms, were 44.1 and 55.7 mg g^{-1}, respectively (Table 3). Values of the Langmuir constant (k_a) were 0.005 and 0.009 l mg^{-1}, respectively, for activated carbon and irradiation-grafted activated carbon, indicating the affinity of the binding sites to binding with Ni^{2+} ions was higher with the irradiation-grafted activated carbon. This result shows that the capacity for nickel adsorption by both adsorbents is dependent mainly on the number of the functional groups on their surfaces.

4.4. Desorption

The results from the Ni desorption experiments are presented in Table 4. With both adsorbents <1% of the Ni was released by water,

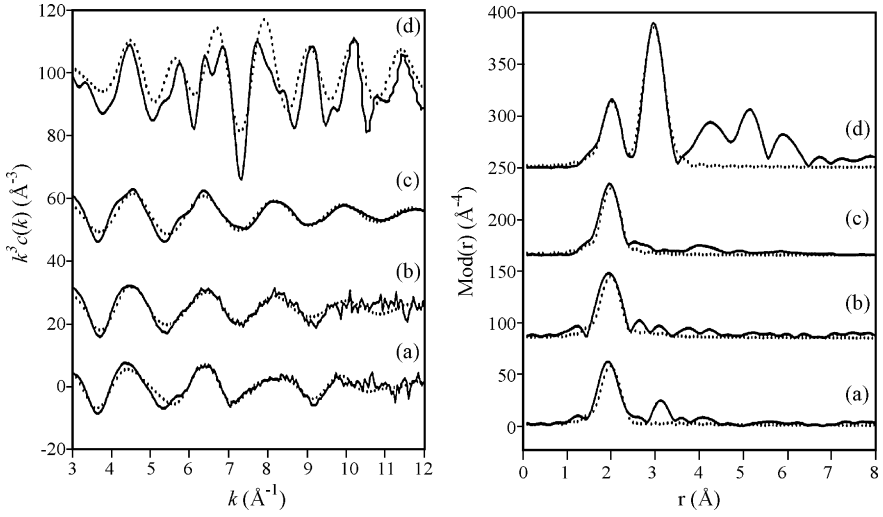

Fig. 5. Experimental (solid line) and calculated (dotted line) EXAFS functions (left) and their Fourier transforms (right) of nickel adsorbed on (a) activated carbon, (b) irradiation-grafted activated carbon, (c) $NiSO_4{\cdot}6H_2O$, and (d) NiO (black).

but ~97% was desorbed with dilute H_2SO_4, the electronegativity value of H^+ ions (EN. H^+ is 2.20) were able to replace Ni^{2+} ions (EN. Ni^{2+} is 1.91) indicating that nickel adsorption on activated carbon and irradiation-grafted activated carbon involves an ion exchange mechanism.

4.5. X-ray absorption spectroscopy (XAS)

X-ray absorption spectroscopy (XAS) was used to characterize the chemical state and environment of the Ni. X-ray absorption near edge structure (XANES) provided information on the coordination geometry and oxidation state of the metal, whereas X-ray absorption fine structure (EXAFS) data contain information about the backscattering atoms, coordination numbers and bond distances.

Fig. 4 shows the XANES spectra of nickel adsorbed on activated carbon and irradiation-grafted activated carbon along with reference samples nickel foil, NiO (black) and $NiSO_4{\cdot}6H_2O$. The absorption edge energies indicate that nickel is in the +2 oxidation state and contains octahedral coordination.

The k^3-weighted EXAFS functions and the corresponding Fourier transforms for all of the samples are reported in Fig. 5, and the structural parameters summarized in Table 5. Fitting NiO and $NiSO_4{\cdot}6H_2O$ with an octahedral oxygen coordination produced a first shell at a distance of about 2.07 Å [34,35], while the spectrum of Ni adsorbed on activated carbon and irradiation-grafted activated carbon could be fitted with oxygen shell at a distance of about 2.04–2.06 Å and a coordination number of 6.

A second shell could be fitted with carbon atoms at distances ranging from 2.95 to 3.09 Å, which are similar distance of Ni–C in $NiCO_3$ [36]. The signal from this shell was very weak signal and it was not possible to determine the number of carbon atoms.

5. Conclusion

Adsorption of nickel on activated carbon could be increased by grafting sodium polyacrylate using γ-irradiation. Desorption, FTIR and XAS studies indicate that the adsorbed Ni was bound to 6 oxygen atoms from carboxyl groups at a distance of 2.04–2.06 Å in first shell. From this result shows the grafting technique with gamma rays, could be applied to other polymers in order to increase metal adsorption capacity. This technique will help the treatment of industrial wastewater economical.

Acknowledgements

The authors would like to thank the National Synchrotron Research Center for support this research. Miss Arunee Ewecharoen gratefully acknowledges a Ph.D. Scholarship from the Royal Golden Jubilee Project of the Thailand Research Fund. We would like to thank the Hamburger Synchrotronstrahlungslabor (HASYLAB) at DESY in Hamburg, Germany was for supporting beamtime X1, also like to thank the scientist beamline, Dr. Adam Webb and Beta Gamma Service GmbH & Co. KG, Germany, for gamma rays supported.

References

[1] S. Mohana, B.K. Acharya, D. Madamwar, Distillery spent wash: treatment technologies and potential applications, J. Hazard. Mater. 163 (2009) 12–25.
[2] A.N. Bdour, M.R. Hamdi, Z. Tarawneh, Perspectives on sustainable wastewater treatment technologies and reuse options in the urban areas of the Mediterranean region, Desalination 237 (2009) 162–174.
[3] J. Jaramillo, V. Gómez-Serrano, P.M. Álvarez, Enhanced adsorption of metal ions onto functionalized granular activated carbons prepared from cherry stones, J. Hazard. Mater. 161 (2009) 670–676.
[4] S. Babel, T.A. Kurniawan, Low-cost adsorbents for heavy metals uptake from contaminated water: a review, J. Hazard. Mater. 97 (2003) 219–243.
[5] A. Dabrowski, Adsorption—from theory to practice, Adv. Colloid Interface 93 (2001) 135–224.
[6] I. Villaescusa, N.r. Fiol, M. Martinez, N.r. Miralles, J. Poch, J. Serarols, Removal of copper and nickel ions from aqueous solutions by grape stalks wastes, Water Res. 38 (2004) 992–1002.
[7] J.L. Gardea-Torresdey, K. Dokken, K.J. Tiemann, J.G. Parsons, J. Ramos, N.E. Pingitore, G. Gamez, Infrared and X-ray absorption spectroscopic studies on the mechanism of chromium(III) binding to alfalfa biomass, Microchem. J. 71 (2002) 157–166.
[8] D. Lu, Q. Cao, X. Li, X. Cao, F. Luo, W. Shao, Kinetics and equilibrium of Cu(II) adsorption onto chemically modified orange peel cellulose biosorbents, Hydrometallurgy 95 (2009) 145–152.
[9] N. Toumi, I. Bonnamour, J.P. Joly, G. Finqueneisel, L. Retailleau, R. Kalfat, R. Lamartine, Grafting of calix[4]arene derivative on activated carbon surface, Mater. Sci. Eng. C 26 (2006) 490–494.
[10] Y.G. Ko, P.X. Ma, Surface-grafting of phosphates onto a polymer for potential biomimetic functionalization of biomaterials, J. Colloid Interface Sci. 330 (2009) 77–83.
[11] S. Majumdar, J. Dey, B. Adhikari, Taste sensing with polyacrylic acid grafted cellulose membrane, Talanta 69 (2006) 131–139.
[12] F.E. Okieimen, C.E. Sogbaike, J.E. Ebhoaye, Removal of cadmium and copper ions from aqueous solution with cellulose graft copolymers, Sep. Purif. Technol. 44 (2005) 85–89.
[13] V. Singh, P. Kumari, S. Pandey, T. Narayan, Removal of chromium (VI) using poly(methylacrylate) functionalized guar gum, Bioresour. Technol. 100 (2009) 1977–1982.
[14] D. He, H. Susanto, M. Ulbricht, Photo-irradiation for preparation, modification and stimulation of polymeric membranes, Prog. Polym. Sci. 34 (2009) 62–98.
[15] J. Deng, L. Wang, L. Liu, W. Yang, Developments and new applications of UV-induced surface graft polymerizations, Prog. Polym. Sci. 34 (2009) 156–193.
[16] M.F. Abou Taleb, G.A. Mahmoud, S.M. Elsigeny, E.-S.A. Hegazy, Adsorption and desorption of phosphate and nitrate ions using quaternary (polypropylene-g-N,N-dimethylamino ethylmethacrylate) graft copolymer, J. Hazard. Mater. 159 (2008) 372–379.
[17] Y.H. Gad, Preparation and characterization of poly(2-acrylamido-2-methylpropane-sulfonic acid)/chitosan hydrogel using gamma irradiation and its application in wastewater treatment, Radiat. Phys. Chem. 77 (2008) 1101–1107.
[18] H. Hasar, Adsorption of nickel(II) from aqueous solution onto activated carbon prepared from almond husk, J. Hazard. Mater. 97 (2003) 49–57.
[19] H. Lata, V.K. Garg, R.K. Gupta, Sequestration of nickel from aqueous solution onto activated carbon prepared from *Parthenium hysterophorus* L., J. Hazard. Mater. 157 (2008) 503–509.
[20] L. Monser, N. Adhoum, Modified activated carbon for the removal of copper, zinc, chromium and cyanide from wastewater, Sep. Purif. Technol. 26 (2002) 137–146.
[21] S. Zhu, N. Yang, D. Zhang, Poly(N,N-dimethylaminoethyl methacrylate) modification of activated carbon for copper ions removal, Mater. Chem. Phys. 113 (2009) 784–789.
[22] J.W. Choi, K.S. Yang, D.J. Kim, C.E. Lee, Adsorption of zinc and toluene by alginate complex impregnated with zeolite and activated carbon, Curr. Appl. Phys. 9 (2009) 694–697.
[23] R.R. Dash, C. Balomajumder, A. Kumar, Removal of cyanide from water and wastewater using granular activated carbon, Chem. Eng. J. 146 (2009) 408–413.
[24] A.E. Nemr, O. Abdelwahab, A. El-Sikaily, A. Khaled, Removal of direct blue-86 from aqueous solution by new activated carbon developed from orange peel, J. Hazard. Mater. 161 (2009) 102–110.
[25] S. Azizian, M. Haerifar, H. Bashiri, Adsorption of methyl violet onto granular activated carbon: equilibrium, kinetics and modeling, Chem. Eng. J. 146 (2009) 36–41.
[26] B. Sen Gupta, M. Curran, S. Hasan, T.K. Ghosh, Adsorption characteristics of Cu and Ni on Irish peat moss, J. Environ. Manage. 90 (2009) 954–960.
[27] A. Ewecharoen, P. Thiravetyan, W. Nakbanpote, Comparison of nickel adsorption from electroplating rinse water by coir pith and modified coir pith, Chem. Eng. J. 137 (2008) 181–188.
[28] R.S. Mikhail, S. Brunauer, Surface area measurements by nitrogen and argon adsorption, J. Colloid Interface Sci. 52 (1975) 572–577.
[29] H.P. Boehm, Surface oxides on carbon and their analysis: a critical assessment, Carbon 40 (2002) 145–149.
[30] M. Newville, IFEFFIT: interactive XAFS analysis and FEFF fitting, J. Synchrotron Radiat. 8 (2001) 322–324.
[31] B. Ravel, M. Newville, Athena, artemis, hephaestus: data analysis for X-ray absorption spectroscopy using IFEFFIT, J. Synchrotron Radiat. (2005) 537–541.
[32] M. Newville, P. Livins, Y. Yacoby, J.J. Rehr, E.A. Stern, Near-edge X-ray-absorption fine structure of Pb: a comparison of theory and experiment, Phys. Rev. B 47 (1993) 14126–14131.
[33] S.J. Gurman, N. Binsted, I. Ross, A rapid, exact, curved-wave theory for EXAFS calculations. II. The multiple-scattering contributions, J. Phys. C: Solid State 19 (1986) 1845–1861.
[34] S. Sasaki, K. Fujino, Y. Takeuchi, X-ray determination of electron-density distributions in oxides, MgO, MnO, CoO, and NiO, and atomic scattering factors of their constituent atoms, P. Jpn. Acad. B-Phys. 55 (1979) 43–48.
[35] C.A. Beevers, H. Lipson, The crystal structure of nickel sulphate hexahydrate $NiSO_4{\cdot}(H_2O)_6$, Z. Kristallogr. 83 (1932) 123–135.
[36] F. Pertlik, Structures of hydrothermally synthesized cobalt(II) carbonate and nickel(II) carbonate, Acta Crystallogr. C 42 (1986) 4–5.